ISSN 1063-7761, Journal of Experimental and Theoretical Physics, 2014, Vol. 118, No. 6, pp. 959–970. © Pleiades Publishing, Inc., 2014.
Original Russian Text © V.V. Val'kov, D.M. Dzebisashvili, A.F. Barabanov, 2014, published in Zhurnal Eksperimental'noi i Teoreticheskoi Fiziki, 2014, Vol. 145, No. 6, pp. 1087–1100.

ELECTRONIC PROPERTIES OF SOLID

Effect of the Concentration-Dependent Spin–Charge Correlations on the Evolution of the Energy Structure of the 2D Emery Model

V. V. Val'kov[a], D. M. Dzebisashvili[a,b], and A. F. Barabanov[c]

[a] *Kirensky Institute of Physics, Siberian Branch, Russian Academy of Sciences, Krasnoyarsk, 660036 Russia*
[b] *Siberian State Aerospace University, Krasnoyarsk, 660014 Russia*
[c] *Institute of High-Pressure Physics, Russian Academy of Sciences, Troitsk, Moscow, 142190 Russia*
e-mail: vvv@iph.krasn.ru; ddm@iph.krasn.ru

Received January 12, 2014

Abstract—It is shown using the 2D Emery model that the strong coupling between the spin subsystem of copper ions in the singlet state and the subsystem of oxygen holes considerably reduces the spectral intensity of the correlation function for holes on the Fermi contour. Spin–charge correlations are manifested in the existence of two channels. The first channel is due to the p–d exchange coupling of spins of the oxygen and copper holes. The second channel appears as a result of spin-correlated hoppings, when the motion of holes over oxygen ions is accompanied by spin-flip processes (i.e., simultaneous changes in the spin projections of an oxygen hole and a copper ion). It is established as a result of self-consistent calculations that the allowance for the concentration dependence of spin correlators and multicenter spin–charge correlators appearing in the dispersion equation ensures a decrease in the energy of the system and considerably affects the evolution of the Fermi surface under hole doping.

DOI: 10.1134/S1063776114060223

1. INTRODUCTION

It is assumed that the energy spectrum of Fermi excitations of the normal phase of high-T_c superconductors forms under the mutual influence of the spin and charge degrees of freedom [1–9]. Its origin in the effective Emery model [10–12] with two oxygen ions per unit cell is associated with a large exchange coupling between the spins of oxygen holes and copper holes [13]. An important feature of this interaction is that it leads to spin-correlated hoppings [2, 3, 14], i.e., to hoppings accompanied by spin-flip processes. As a result, the charge transfer with a simultaneous change in the spin moment projection of an oxygen hole begins to play an important role. In accordance with the law of conservation of the total projection of the spin moment of the entire system, a change in the spin projection of a hole on a copper ion is initiated.

It is well known that the spin-polaron concept makes it possible to obtain a correct description of short-range correlations in constructimg the theory of the energy structure of the 2D Emery model [2, 3]. With such an approach, strong spin–charge fluctuations are taken into account by extending the basis set of operators, which includes the multiplicative operators defined as the product of spin and Fermi operators pertaining to neighboring sites. Then the construction of the equations of motion for the set of the basis operators introduced in this way with the subsequent application of the Zwanzig–Mori projection method [4–6, 15, 16] makes it possible to rigorously and self-consistently take into account the short-range spin–fermion correlations, because the decoupling procedure is not used for multiplicative operators. As a result, the Fermi excitation spectrum acquires a dependence on spin–fermion correlations, which substantially affects the concentration-dependent evolution of the Fermi contour.

Experimental investigations of angle-resolved photoemission spectroscopy (ARPES) indicate that the rigid-band model is inapplicable for describing the observed transformation of the Fermi surface (FS) upon an increase in the hole concentration in the system [17–21]. In particular, it is found that the Fermi excitation spectrum in optimally doped cuprates differs significantly from the spectrum of cuprate insulators. In undoped compounds, an isotropic bottom of the band is observed in the vicinity of point $N = (\pi/2, \pi/2)$ of the momentum space [17, 22–25], while in optimally doped cuprates, there appear a large FS with the center at point $M = (\pi, \pi)$ and the region of a plane band in the form of an extended saddle point in the $(0, \pi/2)$–$(0, \pi)$ direction [18, 26–31]. For low and intermediate doping levels, the region of the plane band is also observed in the $(0, \pi)$–$(\pi/2, \pi)$ direction. In the case of intermediate doping, a high-energy pseudogap exists near points $X = \{(\pi, 0), (0, \pi)\}$ with an energy on the order of 0.1 eV [23, 32–34].

We will show that the experimentally observed peculiarities in the evolution of the FS [17, 22–25] can easily be explained assuming the spin-polaron origin of Fermi quasiparticles [2]. The formation mechanism of such quasiparticles in cuprate superconductors was demonstrated using the effective Hamiltonian for the three-band model [10–12] taking into account direct oxygen–oxygen hoppings in the CuO_2 plane as well as antiferromagnetic (AFM) exchange interaction between the nearest (I_g) and next-to-nearest (I_d) neighbors. It is significant that in constructing the spectrum of hole excitations and in calculating the FS, the actual structure of the CuO_2 plane, as well as the existence of a strong coupling between the spins of copper ions and oxygen holes, is taken into account.

To describe the magnetic subsystem of the CuO_2 plane in La_2CuO_4, we use the results obtained for a 2D AFM-frustrated Heisenberg model with $S = 1/2$. It is well known that the AFM interaction between the nearest spins of Cu^{2+} ions in the CuO_2 plane is strong (on the order of 0.13 eV ≈ 1500 K for La_2CuO_4 [35]) and considerably exceeds the interplanar exchange. The interplanar exchange is mainly responsible for the long-range order observed in the dielectric phase of CuO_2 planes (the characteristic Néel temperature for La_2CuO_4 is $T_N \sim 300$ K). However, even for a comparatively low doping level in the system by holes, the long-range AFM order disappears in the entire temperature range. Such a behavior is successfully simulated by introducing frustration [36]. Cluster calculations indicate a quite large frustration parameter $I_d/I_g \sim 0.1$ even for undoped LSCO [37]. Quantitative analysis of the spin subsystem is carried out using the spherically symmetric self-consistent theory [38–40].

It will be shown that in contrast to the model with a large number of fitting parameters, the transformation of the Fermi contour in our case occurs for two reasons. The first reason is associated with a strong correlation between the subsystem of localized spins of copper ions in the state of a quantum spin liquid and the subsystem of oxygen holes. The second reason is associated with a change in the correlation characteristics of the quantum spin liquid, which appear upon an increase in the doping level.

The article has the following structure. In Section 2, the effective Hamiltonian of the Emery model is presented for the regime of strong but finite Coulomb repulsion between two holes on a copper ion. This Hamiltonian acts in the subspace of homeopolar states of copper ions and describes the strong coupling of localized spin moments and doped holes. In Section 3, the method for calculating the spectral and thermodynamic properties of the system under investigation is considered. Section 4 is devoted to describing the operator basis, which makes it possible to take into account rigorously the short-range spin–charge fluctuations and to determine the excitation spectrum of spin-polaron quasiparticles. The same section presents the equations of motion for the basis operators; as well, we analyze the multicenter spin–charge correlators that play the key role in the formation mechanism of the concentration dependence of the quasiparticle excitation spectra of the spin-polaron ensemble. Section 5 contains the results of self-consistent numerical calculations of the concentration dependence of the spin–charge correlation functions; the effect of these correlators on the evolution of the energy spectrum of Fermi quasiparticles in cuprate superconductors is discussed. The main conclusions following from the results are formulated in Section 6.

2. EFFECTIVE HAMILTONIAN OF THE MODEL

In the regime of strong electron correlations, the three-band p–d model [10–12] can be represented by the effective Hamiltonian [3, 13]

$$\hat{\mathcal{H}} = N(\varepsilon_d - 4\tau) + \varepsilon_p \sum_l c_l^\dagger c_l - t \sum_{l\rho} c_l^\dagger c_{l+\rho} + \sum_{f\delta\delta'} c_{f+\delta}^\dagger \left[\frac{\tau_-}{2} + \tilde{S}_f \tau_+ \right] c_{f+\delta'} + \hat{\mathcal{H}}_{\text{exch}}, \quad (1)$$

where

$$\tau_\pm = \tau(1 \pm \eta), \quad \tau = \frac{(t_{pd})^2}{\Delta_{pd}},$$

$$\eta = \frac{\Delta_{pd}}{U_d - \Delta_{pd}}, \quad \tilde{S}_f = \mathbf{S}_f \cdot \boldsymbol{\sigma}.$$

The first term of this Hamiltonian denotes the energy ε_d of homeopolar states of copper ions, reduced by 4τ due to effects of covalence with four nearest oxygen ions. The degree of mixing of oxygen p- and copper d-orbitals is determined by hybridization parameter t_{pd} and dielectric gap width $\Delta_{pd} = \varepsilon_p - \varepsilon_d$ with charge transfer, which is equal to the difference between the hole energy ε_p at the oxygen ion and ε_d at the copper ion; N is the number of copper sites in the CuO_2 plane, which is equal to the number of unit cells.

The second term in formula (1) describes the binding energy of a doped hole with an oxygen ion. Operators $c_l^\dagger = (c_{l\uparrow}^\dagger, c_{l\downarrow}^\dagger)$ in the spinor representation correspond to the hole creation operators with projection $\sigma = \pm 1/2$ of spin moments on an oxygen ion at the lth site.

The third term in $\hat{\mathcal{H}}$ corresponds to direct hole hoppings between the nearest oxygen ions connected by vectors ρ. The hopping intensity is determined by the tunneling integral $t > 0$. We will henceforth assume that hybridization parameter t_{pd} exceeds the tunneling integral ($t_{pd} > t$).

The origin of the fourth term in effective Hamiltonian (1) is associated with the inclusion of the second-order terms in hybridization parameter t_{pd}. The opera-

tor emerging in this case describes the hoppings of holes between oxygen ions directly adjoining the copper ion. Operator $\tilde{S}_f$ is defined as the scalar product of spin moment vector operator $\mathbf{S}_f$ on the copper ion at the fth site and vector $\boldsymbol{\sigma} = (\sigma^x, \sigma^y, \sigma^z)$ composed from Pauli spin matrices. The main feature of this operator is that it contains the contributions corresponding to hole hoppings that accompany the spin-flip processes. In such hoppings, a correlated change in the spin projection occurs not only at the hole, but also at the copper ion. It will be shown below that allowance for such contributions considerably affects the formation of the structure of the spin-polaron spectrum of elementary excitations and its dependence on the doping level. Vectors δ and δ' independently assume four values $\{\pm a_x, \pm a_y\} = \frac{1}{2}\{\pm g_x, \pm g_y\}$, where $\{\pm g_x, \pm g_y\}$ are the vectors of the nearest neighbors in the copper lattice.

The last term in expression (1) corresponds to the superexchange interaction between the spin moments of copper ions. We will confine further analysis to interaction only between spins within two coordination spheres:

$$\hat{\mathcal{H}}_{\text{exch}} = \frac{I_g}{2}\sum_{fg}\mathbf{S}_f\mathbf{S}_{f+g} + \frac{I_d}{2}\sum_{fd}\mathbf{S}_f\cdot\mathbf{S}_{f+d}. \quad (2)$$

In this expression, I_g denotes the exchange integral for the nearest spins and I_d ($d = \pm g_x, \pm g_y$) is the exchange integral between next-to-nearest spins. It is convenient to express the exchange constants in terms of frustration parameter p and effective exchange I:

$$I_g = (1-p)I, \quad I_d = pI, \quad 0 \le p \le 1, \quad I > 0. \quad (3)$$

Quantity p can be associated with the concentration x of holes per copper atom [41]. This conformity will be used below for describing the modification of the spin subsystem under doping.

In deriving the effective Hamiltonian from the three-band Emery model, we assumed that the Coulomb interaction energy U_d for two holes on a copper ion is the largest energy parameter of the system ($U_d > \Delta_{pd} \gg t_{pd}$). The effect of the Coulomb interaction for two holes at the same oxygen ion, as well as the interaction of oxygen holes and copper holes, was disregarded.

We assume that the subsystem of localized spin moments of copper ions is in the state of a quantum spin liquid. In this case, the spherical symmetry is preserved in the spin space. This means that spin correlation functions $C_r = \langle \mathbf{S}_r\cdot\mathbf{S}_{f+r}\rangle$ satisfy the relations

$$C_r = 3\langle S_f^{x(y,z)}S_{f+r}^{x(y,z)}\rangle. \quad (4)$$

In addition ($\alpha, \beta = \uparrow, \downarrow$), we can write

$$\langle S_f^{x(y,z)}\rangle = 0, \quad \langle \boldsymbol{\sigma}_{\alpha\beta}\cdot\mathbf{S}_f\rangle = 0,$$
$$\langle \boldsymbol{\sigma}_{\alpha\beta}\cdot[\mathbf{S}_f\times\mathbf{S}_m]\rangle = 0. \quad (5)$$

It should be noted that the hopping integrals in the third and fourth terms of Hamiltonian (1) may in fact differ in sign for different directions of hoppings. It can easily be seen that these signs can be taken into account exactly by introducing factors $\exp\{iQ(l-l')\}$, where $Q = (\pi, \pi)$. After unitary transformation $e^{iQl}c_l \longrightarrow c_l$, these factors vanish, and to reconstruct the spectrum, it is sufficient to carry out the shift $k \longrightarrow k + Q$ in the k space at the end of computations.

Below we use the following values of the model parameters: $t_{pd} = 1.3$ eV, $\Delta_{pd} = 3.6$ eV, $U_d = 10.5$ eV, $t = 0.5$ eV, and $I = 0.16$ eV, which correspond to the generally accepted values [14, 42, 43]. In this case, $\tau = 0.47$ eV and $\eta = 0.52$.

3. MORI–ZWANZIG PROJECTION FORMALISM

The problem of describing spin–charge fluctuations can be solved in two stages. The first stage is associated with the derivation of closed equations for the family of two-time Green's functions, in which the spin–charge fluctuations of interest are reflected without using linearization methods. At the second stage, the system of equations for the Green's functions is solved numerically with simultaneous determination of the self-consistent mean values.

The closed system of equations for the two-time Green's functions can be derived using the method of irreducible Green's functions and the Mori–Zwanzig projection formalism [4–6, 15, 16]. Let us consider retarded two-time Green's functions

$$G_{ij}(k,t) = \langle\langle A_{ik}(t)|A_{jk}^{\dagger}(0)\rangle\rangle$$
$$= -i\theta(t)\langle[A_{ik}(t), A_{jk}^{\dagger}(0)]\rangle, \quad (6)$$

where $A_{jk} = N^{-1/2}\sum_f e^{-ikf}A_{jf}$ is the basis set of operators in the momentum representation and A_{jf} ($j = 1, \ldots, n$) are the basis operators in the Wannier representation. The form of these operators, as well as their number n for a fixed value of quasi-momentum k, is determined by the specific features of the problem.

Let us write a system of $n \times n$ equations of motion for the Green's functions introduced above:

$$\omega\langle\langle A_{ik}|A_{jk}^{\dagger}\rangle\rangle_{\omega} = K_{ij} + \langle\langle[A_{ik}, \hat{\mathcal{H}}]|A_{jk}^{\dagger}\rangle\rangle_{\omega}, \quad (7)$$

where quantity K_{ij} is the mean value of the anticommutator of basis operators A_{ik} and $A_{jk}^{\dagger}$:

$$K_{ij} = \langle\{A_{ik}, A_{jk}^{\dagger}\}\rangle. \quad (8)$$

In accordance with the projection method, the Green's functions occurring as a result of commuta-

tion $[A_{ik}, \hat{\mathcal{H}}]$ can be written as a linear superposition of basis Green's functions (6):

$$\langle\langle [A_{ik}, \hat{\mathcal{H}}] | A_{jk}^{\dagger} \rangle\rangle_{\omega} = \sum_{l} L_{il}(k) \langle\langle A_{lk} | A_{jk}^{\dagger} \rangle\rangle_{\omega}, \qquad (9)$$

where

$$L(k) = D(k)K^{-1}, \quad D_{ij}(k) = \langle \{ [A_{ik}, \hat{\mathcal{H}}], A_{jk}^{\dagger} \} \rangle. \qquad (10)$$

The resultant system of equations for the Green's functions $\langle\langle A_{ik} | A_{jk}^{\dagger} \rangle\rangle_{\omega}$ is closed; for brevity, this system can be written in matrix form:

$$(\omega \hat{I} - D(k)K^{-1})G(k, \omega) = K, \qquad (11)$$

where $\hat{I}$ is the unit matrix. In this case, the energy spectrum E_{jk} of quasiparticles is determined by the poles of the Green's function $G(k, \omega)$ and can be obtained from the dispersion equation

$$\det \left| \omega \hat{I} - D(k)K^{-1} \right| = 0. \qquad (12)$$

4. SPIN-POLARON BASIS

The specific form of elements of matrix K_{ij} and energy matrix $D_{ij}(k)$ depends of the choice of basis operators $\{A_{jk}\}$. In analyzing effective Hamiltonian (1) of the Emery model, the minimal set of basis operators taking into account the strong coupling between the subsystem of localized spins of copper ions and the spins of oxygen holes consists of three operators [3]:

$$A_{1f} = c_{f+a_x}, \quad A_{2f} = c_{f+a_y},$$
$$A_{3f} = \frac{1}{2}\tilde{S}_f \sum_{\delta} c_{f+\delta}, \quad \delta = \pm a_x, \pm a_y. \qquad (13)$$

Operator A_{f1} (A_{f2}) annihilates the hole in the fth cell on the oxygen ion at site $f + a_x$ ($f + a_y$) located on the p_x (p_y) orbital. A third operator A_{f3} is introduced to rigorously take into account the spin–fermion correlations. It is written in the form of the product of the spin operator corresponding to the fth cell and the operator written in the form of a linear superposition of four Fermi operators of oxygen holes pertaining to four sites, which are nearest to the fth copper ion. It should be noted that the spinor form of this operator reflects the $SU(2)$ invariance of the Hamiltonian of the system and the spin-liquid state of the spin subsystems of copper ions and oxygen holes. It is noteworthy that the expression for operator A_{f3} used here includes the terms corresponding to the above-mentioned spin-flip processes. All operators in this case are acting in the Hilbert space of states of effective Hamiltonian (1) including only the homeopolar states of copper ions.

The exact equations of motion for basis operators (13) have the form

$$i\frac{dA_{1f\sigma}}{dt} = [A_{1f\sigma}, \hat{\mathcal{H}}] = \varepsilon_p A_{1f\sigma} + \left(\frac{\tau_-}{2} - t\right) \times (A_{2f\sigma} + A_{2,f-g_y,\sigma} + A_{2,f+g_x,\sigma} + A_{2,f+g_x-g_y,\sigma}) + \frac{\tau_-}{2}(2A_{1f\sigma} + A_{1,f-g_x,\sigma} + A_{1,f+g_x,\sigma}) + 2\tau_+(A_{3f\sigma} + A_{3,f+g_x,\sigma}), \qquad (14)$$

$$i\frac{dA_{2f\sigma}}{dt} = [A_{2f\sigma}, \hat{\mathcal{H}}] = \varepsilon_p A_{2f\sigma} + \left(\frac{\tau_-}{2} - t\right) \times (A_{1f\sigma} + A_{1,f-g_x,\sigma} + A_{1,f+g_y,\sigma} + A_{1,f+g_y-g_x,\sigma}) + \frac{\tau_-}{2}(2A_{2f\sigma} + A_{2,f-g_y,\sigma} + A_{2,f+g_y,\sigma}) + 2\tau_+(A_{3f\sigma} + A_{3,f+g_y,\sigma}), \qquad (15)$$

$$i\frac{dA_{3f\sigma}}{dt} = [A_{3f\sigma}, \hat{\mathcal{H}}] = \frac{3}{2}\tau_+ \sum_{\delta} c_{f+\delta,\sigma} + \left(\varepsilon_p - 2t + \frac{5}{2}\tau_- - 4\tau_+\right) A_{3f\sigma} + \left(\frac{\tau_-}{2} - t\right)\frac{1}{2}\sum_{\Delta}(\tilde{S}_f c_{f+\Delta})_{\sigma} + \frac{\tau_-}{4}\sum_{\delta}(\tilde{S}_f c_{f+3\delta})_{\sigma} + \frac{\tau_+}{2}\left[\sum_{\delta\delta'}(\mathbf{S}_f \cdot \mathbf{S}_{f+2\delta'}) c_{f+2\delta'+\delta,\sigma}\right. + i\sum_{\delta\delta'\alpha}\boldsymbol{\sigma}_{\sigma\alpha} \cdot [\mathbf{S}_f \times \mathbf{S}_{f+2\delta'}] c_{f+2\delta'+\delta,\alpha} + \left. i\sum_{\substack{\delta\delta_1\delta' \\ \alpha\beta\gamma}} [\boldsymbol{\sigma}_{\sigma\gamma} \times \boldsymbol{\sigma}_{\alpha\beta}] \cdot \mathbf{S}_f c^{\dagger}_{f+\delta,\alpha} c_{f+\delta_1,\beta} c_{f+\delta',\gamma}\right] + \frac{i}{2}\sum_{\delta n\alpha} I_{fn}\boldsymbol{\sigma}_{\sigma\alpha} \cdot [\mathbf{S}_n \times \mathbf{S}_f] c_{f+\delta,\alpha}, \qquad (16)$$

where Δ is a vector running through eight values: $\{\pm g_x \pm a_y, \pm g_y \pm a_x\}$. This vector connects a copper ion and next-to-nearest oxygen ions. As before, vector δ (δ') assumes four values: $\{\pm a_x, \pm a_y\}$. Note that in contrast to the first two equations (14) and (15), the right-

hand side of the third equation of motion (16) cannot be expressed in terms of basis operators (13). The right-had side of Eq. (16) has acquired new operators with a more complex structure.

Projecting the right-hand sides of Eqs. (14)–(16) onto basis (13), we take advantage of the fact that the spin subsystem is in the state of a quantum spin liquid. This allows us to calculate the elements of matrices $D(k)$ and $K(k)$ using the simplifying assumptions associated with vanishing of mean values (5). Omitting intermediate calculations, we write the final expressions ($D_{ij}(k) = D_{ji}^{*}(k)$ and $K_{ij}(k) = K_{ji}^{*}(k)$):

$$\begin{aligned}
D_{11}(k) &= \varepsilon_p + \tau_-(1+\cos k_x),\\
D_{22}(k) &= \varepsilon_p + \tau_-(1+\cos k_y),\\
D_{31}(k) &= 2\tau_+(1+e^{-ik_x})K_{33},\\
D_{32}(k) &= 2\tau_+(1+e^{-ik_y})K_{33},\\
D_{12}(k) &= \left(\frac{\tau_-}{2}-t\right)(1+e^{ik_x})(1+e^{-ik_y}),\\
D_{33}(k) &= \left(\varepsilon_p - 2t + \frac{5}{2}\tau_- - 4\tau_+\right)K_{33}\\
&+\left(\frac{\tau_-}{2}-t\right)[2C_1\gamma_1(k)+2C_2\gamma_2(k)-M_2]\\
&+\frac{\tau_-}{2}[C_1\gamma_1(k)+C_3\gamma_3(k)-M_3]\\
&+\tau_+\Big[4M_1+C_1(1-4\gamma_1(k))\\
&+\frac{3}{2}(x+8\mathcal{H}_1+4\mathcal{H}_2)-L_1+2Q_1\gamma_1(k)\Big]\\
&+I_g[C_1(\gamma_1(k)-4)-L_1\gamma_1(k)+Q_1]\\
&+I_d[-4C_2-L_2\gamma_2(k)+Q_2];
\end{aligned} \tag{17}$$

$$\begin{aligned}
K_{11} &= K_{22} = 1, \quad K_{12} = K_{13} = K_{23} = 0,\\
K_{33} &= \frac{3}{4} + C_1\gamma_1(k) - M_1.
\end{aligned} \tag{18}$$

It can be seen that the matrix elements can be expressed not only in terms of spin correlators (4) and kinematic correlators $\mathcal{H}_{l-l'}$, but also in terms of the spin–charge correlation functions:

$$\begin{aligned}
M_1 &= \frac{1}{2}\sum_{\delta}\langle A_{3f}^{\dagger}c_{f+\delta}\rangle,\\
M_2 &= \frac{1}{2}\sum_{\Delta}\langle A_{3f}^{\dagger}c_{f+\Delta}\rangle,\\
M_3 &= \frac{1}{2}\sum_{\delta}\langle A_{3f}^{\dagger}c_{f+3\delta}\rangle,
\end{aligned} \tag{19}$$

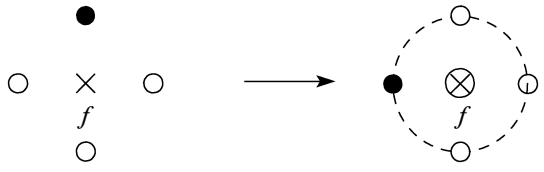

Fig. 1. Diagram of the process of transition of a hole from an oxygen ion at site $f + r$ to the coherent state determined by operator $A_{3f}^{\dagger}$. The amplitude of this process determines the value of correlator M_1. The dark circle in the left part of the figure indicates the oxygen ion on which the hole is located, and light circles show oxygen ions without a hole. The dashed circle connecting four oxygen sites in the right part of the figure illustrates the fact that the hole can equiprobably be at any of the four oxygen ions. The superposition of these states possesses the property of coherence in the phase factors as well in the spin configurations of the copper–oxygen orbitals. The copper ion participating in the correlated spin dynamics is denoted by the crossed circle.

$$\begin{aligned}
L_1 &= 2\sum_{g}\langle A_{3,f+g,\sigma}^{\dagger}A_{3f\sigma}\rangle,\\
L_2 &= 2\sum_{d}\langle A_{3,f+d,\sigma}^{\dagger}A_{3f\sigma}\rangle,
\end{aligned} \tag{20}$$

$$\begin{aligned}
Q_1 &= \sum_{\delta g}\langle (c_{f+\delta}^{\dagger}\tilde{S}_{f+g})_{\sigma}A_{3f\sigma}\rangle,\\
Q_2 &= \sum_{\delta d}\langle (c_{f+\delta}^{\dagger}\tilde{S}_{f+d})_{\sigma}A_{3f\sigma}\rangle,
\end{aligned} \tag{21}$$

in which vector g assumes four values $\pm g_{x(y)}$ from the first coordination sphere for the sublattice of copper ions and vector d assumes four values $\pm g_x \pm g_y$ from the second coordination sphere for the same sublattice. In further analysis, from the entire set of kinematic correlators

$$\mathcal{H}_{l-l'} = \langle c_{l\sigma}^{\dagger}c_{l'\sigma}\rangle \tag{22}$$

we will use only two ($\mathcal{H}_{l-l'} = \mathcal{H}_1$ if l and l' are the indices of the nearest oxygen ions and $\mathcal{H}_{l-l'} = \mathcal{H}_2$ if l and l' are the indices of the next-to-nearest sites in the oxygen lattice).

Since spin–charge correlators (19)–(21) are important for calculating the concentration-dependent evolution of the spectrum of spin-polaron quasiparticles, the meaning of these correlators is illustrated in Figs. 1–3.

The spin–charge correlators M_j ($j = 1, 2, 3$) in formula (19) describe the averaged probability amplitude of the transition of a hole from the p state on the oxygen ion with number $f + r$ to a coherent state described by superposition of the p states of a hole on four oxygen ions nearest to site f, which correlate with the copper ion in spin variables. Correlator M_1 (see Fig. 1)

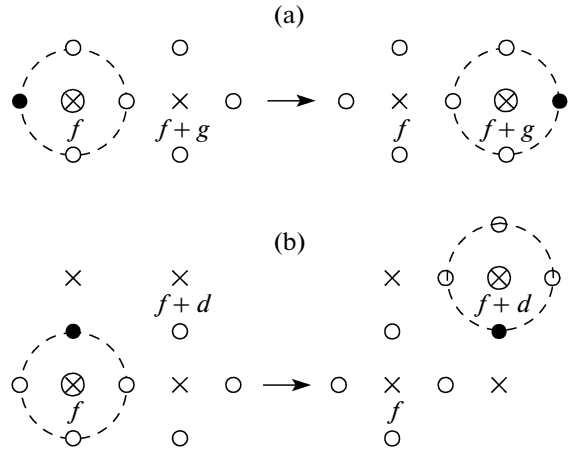

Fig. 2. Diagrams of the processes determining correlation functions L_1 and L_2. Prior to the transition, the coherent superposition of one-hole states corresponded to site f; after the transition, it corresponds to site $f + g$ (a) or $f + d$ (b). The remaining notation is the same as in Fig. 1.

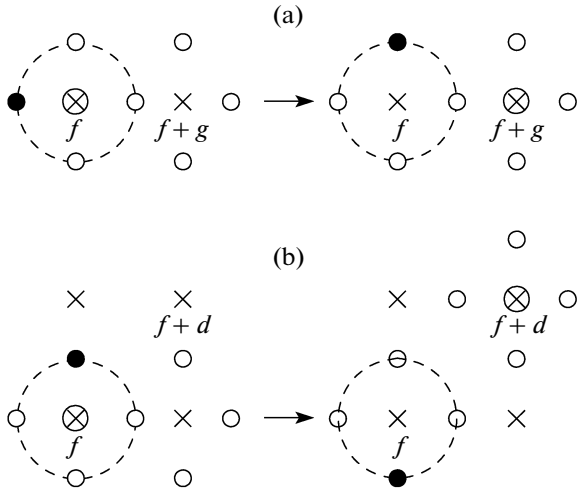

Fig. 3. Diagrams of the processes determining correlation functions Q_1 and Q_2. In the initial state, the spin–charge coherence was formed relative to site f. In the final state, the charge coherence relative to site f is preserved, while the spin coherence is formed relative to site $f + g$ (for the process determining correlator Q_1) or relative to site $f + d$ (for the process determining correlator Q_2). The remaining notation is the same as in the previous figures.

corresponds to $r = \delta$. Correlator M_2 (M_3) has the same physical meaning as correlator M_1, the only difference being that a transition of a hole to the above coherent state occurs from a site located in the second ($r = \Delta$) (third, $r = 2\delta$) coordination sphere.

In contrast to M_1 (M_2), correlation function L_1 (L_2) describes the probability amplitude of the transition of a hole not from a fixed oxygen ion, but from the above coherent superposition (pertaining to site f) to a coherent superposition of states pertaining to the nearest (next-to-nearest) site $f + g$ ($f + d$) of a copper ion. Figures 2a and 2b schematically illustrate such an interpretation.

Correlators Q_1 and Q_2 (21) reflect the averaged amplitudes of the processes in which it is not charge transfer that takes place, but the spin partner participating in the formation of the spin-coherent states changes: for correlator Q_1, the spin partner is the copper ion at site $f + g$, while the spin partner for correlator Q_2 is the copper ion at site $f + d$. The corresponding processes are illustrated in Fig. 3.

All spin–fermion correlators appearing in the theory can be calculated using the spectral theorem applied to the corresponding Green's functions. For these functions, the system of closed equations can be written using the above equations of motion. To calculate kinematic correlators (22), we must use Green's functions $G_{11}(k, \omega)$ and $G_{12}(k, \omega)$. To determine spin–charge correlators M_j ($j = 1, 2, 3$), the Green's function $G_{13}(k, \omega)$ is used, while the Green's function used for calculating correlators L_j ($j = 1, 2$) is $G_{33}(k, \omega)$.

The set of basis operators (13) introduced above is insufficient for calculating correlators Q_j ($j = 1, 2$). If, however, we introduce additional operators

$$A_{4f\sigma} = \frac{1}{2}\sum_{\delta}(\tilde{S}_{f+g_x}c_{f+\delta})_\sigma,$$
$$A_{5f\sigma} = \frac{1}{2}\sum_{\delta}(\tilde{S}_{f+d}c_{f+\delta})_\sigma, \quad (23)$$

and calculate Green's functions $G_{34}(k, \omega) = \langle\langle A_{3k\sigma}|A^\dagger_{4k\sigma}\rangle\rangle_\omega$ and $G_{35}(k, \omega) = \langle\langle A_{3k\sigma}|A^\dagger_{5k\sigma}\rangle\rangle_\omega$, we can easily find correlators Q_j ($j = 1, 2$).

In writing the equations of motion for Green's functions $G_{34}(k, \omega)$ and $G_{35}(k, \omega)$, commutator $[A_3, \hat{\mathcal{H}}]$ will be projected, as before, onto initial basis (13). In this case, there is no need to calculate new matrix elements of energy matrix $D(k)$. All we need to additionally obtain correlators Q_j ($j = 1, 2$) are the matrix elements

$$\langle\{A_{3k}, A^\dagger_{4k}\}\rangle = C_1 + \frac{1}{4}\gamma_1(k)\left[\frac{3}{4} + 2C_2 + C_3 - M_1 - M_2 - M_3\right], \quad (24)$$

$$\langle\{A_{3k}, A^\dagger_{5k}\}\rangle = C_2 + \frac{1}{2}\gamma_1(k)[C_1 + C_4] - \frac{1}{4}\gamma_2(k)[M_2 + M_4]. \quad (25)$$

5. RESULTS OF NUMERICAL CALCULATION OF CORRELATION FUNCTIONS AND ENERGY SPECTRUM

To calculate the energy structure of spin-polaron quasiparticles self-consistently, we must know, apart from the spin–charge and kinematic correlators, the concentration dependence of pair spin correlation functions (4) for three coordinate spheres: C_1 for $r = g$; C_2 for $r = d$, and C_3 for $r = 2g$. These correlation functions C_1, C_2, and C_3, as well as gap $\Delta_Q(p)$ in the magnetic excitation spectrum in the vicinity of point $Q = (\pi, \pi)$ of the Brillouin zone, can be calculated using the spherically symmetric self-consistent approach for a frustrated antiferromagnet (see [44] and literature cited therein). In this case, Δ_Q is a linear function of inverse magnetic correlation length ξ^{-1}. On the other hand, according to the neutron scattering and nuclear magnetic resonance data (see, e.g., [45, 46]), ξ^{-1} is determined by doping level x and increases for LSCO by several times with increasing x in the interval 0.03–0.3. Accordingly, the values of frustrations introduced above (see table) correspond to the case when the spin gap increases by a factor of 2.5 upon an increase in p from 0.15 to 0.3.

The table contains the spin correlators calculated according to this technique for five parameters of frustrartion p. Henceforth, we will assume that these values correspond to five values of hole concentration x.

All the parameters of the problem were calculated self-consistently as follows. For a given doping level x, the values of spin correlators C_j ($j = 1, 2, 3$) were determined from the table. Then nine correlations functions M_j ($j = 1, 2, 3$), $\mathcal{K}_j$, L_j, and Q_j ($j = 1, 2$) were calculated by iterations. At each iteration step, chemical potential μ was determined by solving the equation determining the total concentration of oxygen holes.

The results of self-consistent numerical calculations of correlation functions are shown in Fig. 4. It can be seen that in the absence of doping ($x = 0$), all functions shown in Fig. 4 vanish as expected. Upon doping, the values of these functions increase in absolute value. This increase is especially strong for functions M_1, M_2 and L_1, L_2. Such a behavior leads to a considerable modification of the excitation spectrum of spin-polaron states. It should be noted that in the approximation of a single oxygen hole, all these correlators are disregarded.

The dependence of the dispersion curve for spin-polaron excitations from spin–charge correlations is determined exclusively by matrix elements $D_{33}(k)$ and

Doping levels x and corresponding values of frustration parameter p and spin correlation functions

x	p	C_1	C_2	C_3
0.03	0.15	–0.287	0.124	0.0950
0.07	0.21	–0.255	0.075	0.0640
0.15	0.25	–0.231	0.036	0.0510
0.22	0.275	–0.214	0.009	0.0450
0.30	0.30	–0.194	–0.0222	0.0457

K_{33}. This can easily be seen if we write dispersion equation (12) in explicit form:

$$\begin{aligned}(\omega-\varepsilon_p)^3-(\omega-\varepsilon_p)^2\{2\tau_-(1+\gamma_1(k))+\Lambda(k)\}\\ +(\omega-\varepsilon_p)\{[2\tau_-\Lambda(k)-16\tau_+^2K_{33}](1+\gamma_1(k))\\ +4t(\tau_--t)\chi(k)\}\\ +4t\chi(k)[8\tau_+^2K_{33}-\Lambda(k)(\tau_--t)]=0,\end{aligned} \tag{26}$$

where the following functions have been introduced for brevity:

$$\Lambda(k)=\frac{D_{33}(k)}{K_{33}}-\varepsilon_p,\quad \chi(k)=1+2\gamma_1(k)+\gamma_2(k).$$

Here and below, we use standard notation for the invariants of the square lattice:

$$\gamma_1(k)=\frac{1}{2}(\cos(k_x)+\cos(k_y)),$$

$$\gamma_2(k)=\cos(k_x)\cos(k_y),$$

$$\gamma_3(k)=\frac{1}{2}(\cos(2k_x)+\cos(2k_y)).$$

In the region of hole doping under investigation, spin-polaron excitation spectrum E_{1k} is determined for each value of the quasi-momentum by solving cubic dispersion equation (26) with the lowest values of energy.

If the integral t of direct oxygen–oxygen hoppings is equal to zero, expression (26) is considerably simplified and assumes the form

$$\begin{aligned}[(\omega-\varepsilon_p)^2-(\omega-\varepsilon_p)\{2\tau_-(1+\gamma_1(k))+\Lambda(k)\}\\ +(2\tau_-\Lambda(k)-16\tau_+^2K_{33})(1+\gamma_1(k))](\omega-\varepsilon_p)=0.\end{aligned} \tag{27}$$

It can be seen that in this case, one of the roots of the cubic equation, which generates dispersion level ε_p, splits off. This level corresponds to the unbound oxygen orbital. From this it follows that the admixture of this orbital to spin-polaron states is due only to p–p tunneling.

Figure 5 shows the modification of the dispersion relation of spin-polaron excitations upon a change in hole concentration x. It can be seen that for low dop-

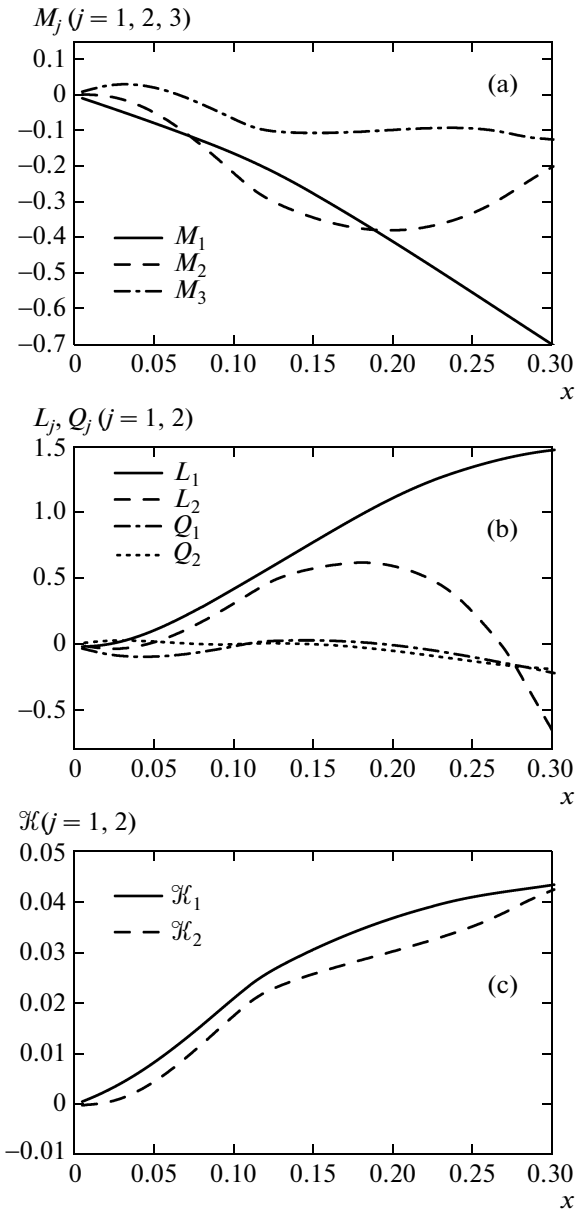

Fig. 4. Concentration dependences of correlation functions: (a) M_j (j = 1, 2, 3); (b) L_j and Q_j (j = 1, 2), and (c) $\mathcal{H}_j$ (j = 1, 2).

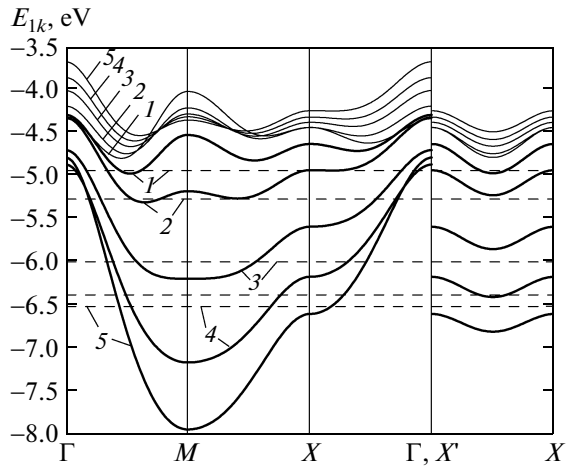

Fig. 5. Dispersion curves for the lower spin-polaron band. Bold curves are calculated taking into account all correlation functions for five values of the doping level: curve *1* for $x = 0.03$; *2* for $x = 0.07$; *3* for $x = 0.15$, *4* for $x = 0.22$, and *5* for $x = 0.3$. Dashed lines denote the positions of the chemical potential for corresponding concentration x. Fine curves are the dispersion curves calculated for the same five values of x taking into account only spin correlators C_j (all spin–charge correlation functions M_j, L_j, Q_j, and $\mathcal{H}_j$ were assumed to be zero).

ing levels $x = 0.03$ and 0.07 (bold curves *1* and *2* in Fig. 5), the Fermi surface forms a hole pocket in the vicinity of point $(\pi/2, \pi/2)$ of the Brillouin zone. As noted in [47], the physical reason for the dispersion minimum in the vicinity of this point is associated with antiferromagnetic fluctuations manifested in spin correlation functions C_j.

Upon an increase in hole concentration x, the spin–charge correlators rapidly increase to the values for which the role of magnetic correlators becomes insignificant. The width of the spin-polaron band increases in this case, and the dispersion minimum shifts to point $M(\pi, \pi)$ of the Brillouin zone. This result is clearly demonstrated by the bold curves *3*–*5* in Fig. 5.

It should be noted that if we disregard the spin–charge correlators, the minimum of the dispersion relation is shifted upon doping only slightly in the direction of point M of the Brillouin zone, but remains at an appreciable distance from it. Such a behavior is depicted by the thin curves in Fig. 5, which describe the evolution of the band structure of spin polarons upon doping in the absence of spin–charge correlations (i.e., in the case when all correlation functions M_j, L_j, Q_j, and $\mathcal{H}_j$ are equal to zero,

Another important effect observed when spin–charge correlators are taken into account is a considerable decrease in the energy of polaron states, which can easily be traced by comparing the bold and fine curves in Fig. 5. The dispersion curves calculated with allowance for spin–charge correlations (bold curves in Fig. 5) are noticeably shifted downwards on the energy scale upon an increase in the doping level, while the dispersion relations calculated without taking into account spin–charge correlators (fine curves in Fig. 5) are shifted upwards.

Such a behavior of the one-particle spectrum of Fermi excitations should obviously affect the behavior of the total energy $E = \langle \hat{\mathcal{H}} \rangle$ of the system, which can be written in the form

$$E = \varepsilon_d + 4\tau + x\varepsilon_p - 16t\mathcal{H}_1 + 4\tau_-(x/4 + 2\mathcal{H}_1 + \mathcal{H}_2) + 4\tau_+ M_1 + 2(I_1C_1 + I_2C_2). \quad (28)$$

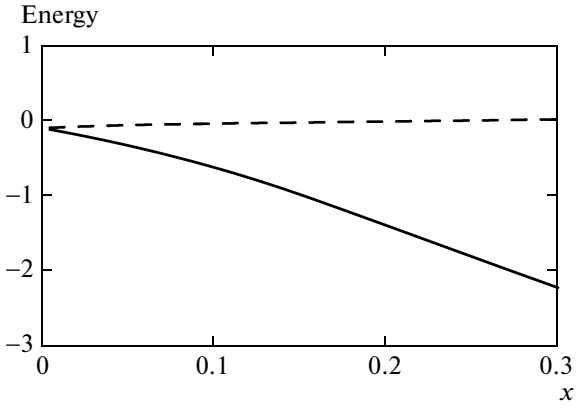

Fig. 6. Concentration dependences of the total energy: the solid curve was calculated taking into account spin–charge correlators M_j, L_j, Q_j, and $\mathcal{H}_j$, while the dashed line was calculated disregarding these correlators.

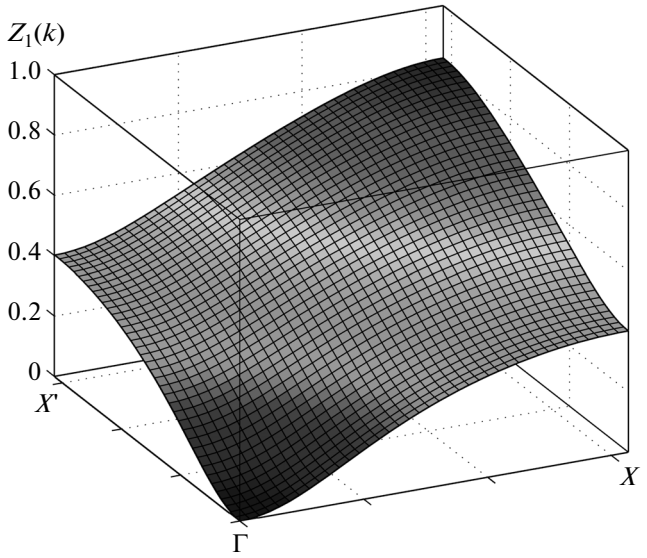

Fig. 7. Spectral density of bare holes for the lower band of spin polarons as a function of the quasi-momentum in the first quarter of the Brillouin zone. Calculations were performed for $x = 0.03$.

The dependence of total energy E of the system on doping level x is shown by the solid curve in Fig. 6. For comparison, the dashed curve in this figure shows the dependence of the total energy calculated disregarding the spin–charge correlators. It can be seen that if correlators M_j, L_j, and Q_j are ignored, energy E increases with hole concentration x. When the spin–charge correlators are taken into account, the total energy of the system decreases with increasing x. It follows from expression (28) and the curves in Fig. 4 that the decrease in energy E is mainly due to correlator M_1.

An important feature of the spin-polaron approach to describing the spectral properties of high-temperature superconductors is associated with a substantial decrease in the spectral density of quasiparticles in the lower spin-polaron band. It should be noted that it is this feature of the spectral intensity that ensures a large FS for optimally doped and overdoped cuprate HTSCs in spite of the fact that the hole concentration in the CuO_2 plane is relatively low in this case.

Figure 7 shows the spectral intensity $Z_1(k)$ of bare holes, which corresponds to the lower band of spin polarons. Its behavior can be determined from the expression for Green's function $G_h(k, \omega)$:

$$G_h(k, \omega) = \sum_{j=1}^{2} \langle\langle A_{jk} | A_{jk}^{\dagger} \rangle\rangle_{\omega} = \frac{Z_1(k)}{\omega - E_{1k}}. \qquad (29)$$

The vanishing of function $Z_1(k)$ at point Γ of the Brillouin zone corresponds, in particular, to the result obtained in [48] from an analysis of the spin-fermion model in the one-hole approximation. The maximal value of the spectral intensity (slightly exceeding 0.8) is attained at point M of the Brillouin zone. For conventional fermions, the spectral intensity $Z_1(k)$ would be equal to four for any value of quasi-momentum k.

It should be emphasized that the substantial decrease in the spectral intensity of the correlation function of spin-polaron quasiparticles occurs for a totally different reason than in the Hubbard model. It is well known that renormalization of the spectral intensity for Hubbard fermions is determined by factor $1 - n/2$ and is almost unnoticeable for a low density n of quasiparticles. This is because the strong interaction in the Hubbard model exists between fermions themselves. If the number of fermions is small, the renormalizations of the spectral intensity of the correlation function of the corresponding quasiparticles are also insignificant.

A different situation takes place in the effective Emery model considered here. As noted above, holes strongly interact not with one another, but with the spin subsystem. Since the spin moment in the regime considered here is located at each copper ion, spin-polaron states are formed for any doping level. Since antibound triplet states of the spin of a copper ion and of an oxygen hole are high-energy states, they are almost unpopulated. For this reason, the spectral weight of spin-polaron quasiparticles is determined only by singlet bound states whose number is one-third that of triplet states. This explains the decrease in the spectral intensity of spin-polaron quasiparticles.

As a result, the maximal population of each state in the quasi-momentum space is substantially smaller as compared to the case of free fermions. A quantitative characteristic of the population density of k-states can be parameter P defined as the ratio of the number of holes within the Fermi contour to the number of the k-states of the Brillouin zone, bounded by the Fermi contour. For $P = 1$, each k-state of the Brillouin zone should be filled. In actual practice, $P < 1$, and the smaller the value of P, the "looser" the filling of the k-states by spin-polaron quasiparticles. Figure 8 shows

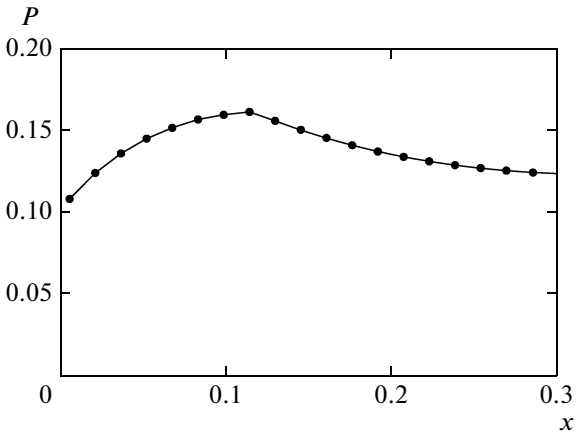

Fig. 8. Concentration dependence of occupancy parameter $P(x)$.

the dependence of parameter P on doping level x. It can be seen that occupation parameter P is much smaller than unity and varies insignificantly in the doping interval $0 < x < 0.3$ under investigation. The nonanalytic behavior of P in the vicinity of $x = x_c \sim 0.12$ is associated with a change in the topology of the structure of Fermi contours, which takes place at x_c.

An important characteristic determining the low-temperature thermodynamics of the quasiparticle ensemble is the density of states. Figure 9 shows the variation of the density of states upon doping. It can be seen that at low values of hole concentration x, there are two Van Hove singularities located above chemical potential μ on the energy scale. As the value of x increases in the interval [0.03, 0.3] under investigation, the chemical potential passes sequentially through the two singularities. For large values of doping level, the lower singularity disappears, and only one Van Hove singularity is preserved. Such a dynamics of the relative variation of the chemical potential and the peaks in the density of states is important for describing the superconducting phase of cuprate HTSCs, since it is well known that the maximal superconducting transition temperature in these compounds is attained at a doping level for which the chemical potential is in the vicinity of the Van Hove singularities.

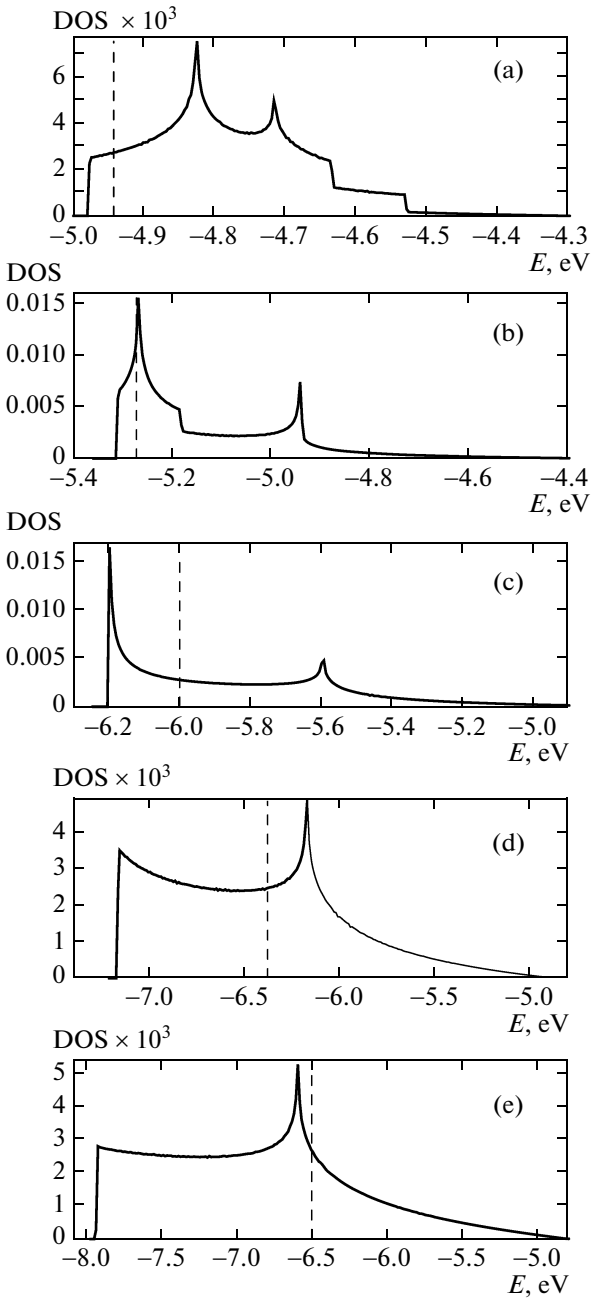

Fig. 9. Evolution of the density of states upon an increase in the hole concentration: (a) $x = 0.03$; (b) $x = 0.07$; (c) $x = 0.15$; (d) $x = 0.22$, and (e) $x = 0.3$. The vertical dashed line denotes the position of the chemical potential.

6. CONCLUSIONS

Our analysis of the structure of Fermi quasiparticles and the energy spectrum in the effective 2D Emery model has led to the following conclusions.

1. Strong spin-fermion correlations between localized spins of copper ions and holes at the nearest oxygen ions form the basis of the spin-polaron origin of Fermi quasiparticles in the CuO_2 plane of HTSCs. The dispersion equation determining the spectrum of the Fermi excitations of such quasiparticles contains functions expressed in terms of multicenter spin and spin-fermion correlators as coefficients. The set of fermion and spin-fermion operators introduced here is sufficient for a self-consistent description of the spin-polaron concept and for calculating the multicenter spin-fermion correlators appearing in the theory.

2. It is found as a result of numerical solution of the self-consistency equation that multicenter spin–charge correlators exhibit a strong concentration dependence. This results in a change in the spectrum

of spin-polaron excitations upon an increase in the number of oxygen holes. We have demonstrated a modification of the energy structure of spin-polaron quasiparticles upon an increase in hole concentration x from a lower doping level $x = 0.03$, for which the Fermi surface forms a small hole pocket in the vicinity of point $(\pi/2, \pi/2)$ of the Brillouin zone, to a high level $x = 0.3$, for which a large Fermi surface is centered at point (π, π) (see Fig. 5). A considerable modification of the density of Fermi states upon an increase in the doping level is observed. At low hole concentrations in the system, the density of states exhibits two Van Hove singularities, while at a higher doping level, there remains only one singularity. This indicates the inapplicability of the rigid-band model for describing the spectrum of Fermi excitations of cuprate superconductors.

3. Spin–charge correlations between the localized spin subsystem and the itinerant fermion system in the effective 2D Emery model cause a significant decrease in the energy of spin-polaron states upon an increase in oxygen hole concentration x. It should be noted in this connection that in the one-hole approximation, the dispersion curves are shifted towards higher energies upon an increase in x.

4. The substantial decrease in the spectral weight of the correlation function for Fermi quasiparticles has a simple spin-polaron origin. In the formation of spin-polaron states, the initial energy level splits into two levels due to the strong exchange coupling between the spins of holes on the copper and oxygen ions. In this case, three triplet states possess a high energy, while one singlet state with a lower energy serves as the basis for the formation of collective spin-polaron quasiparticles. Since the relative weight of singlet states is one-third that of the triplet states, the spectral intensity for lower-lying (i.e., spin-polaron) states decreases when the above-mentioned splitting of the energy level is taken into account and a strong tendency to populate only singlet states is observed.

5. The above conclusions confirm the hypothesis of the spin-polaron origin of Fermi quasiparticles in the normal phase of copper oxides. At the same time, the investigation of Cooper instability in an ensemble of such spin-polaron quasiparticles becomes an urgent problem. It can easily be seen that the approach developed in this study makes it possible indeed to describe the superconducting phase of cuprate HTSCs taking into account the actual structure of the CuO_2 plane and strong spin–fermion correlations. Significantly, Cooper instability is observed in a system of quasiparticles whose energy structure matches the ARPES data. This, however, is beyond the scope of this study and is the object of a separate analysis.

ACKNOWLEDGMENTS

This work was supported by the program "Quantum Physics of Mesoscopic and Disordered Systems" of the Presidium of the Russian Academy of Sciences, the Russian Foundation for Basic Research (project nos. 13-02-00909, 13-02-00523, and 13-02-98013_r-sibir), and the Dynasty foundation.

REFERENCES

1. Yu. A. Izyumov, Phys.—Usp. **40** (5), 445 (1997).
2. A. F. Barabanov, V. M. Berezovskii, E. Zhasinas, and L. A. Maksimov, J. Exp. Theor. Phys. **83** (4), 819 (1996).
3. A. F. Barabanov, R. O. Kuzian, and L. A. Maksimov, Phys. Rev. B: Condens. Matter **55**, 4015 (1997).
4. N. M. Plakida, L. Anton, S. Adam, and G. Adam, J. Exp. Theor. Phys. **97** (2), 331 (2003).
5. A. A. Vladimirov, D. Ihle, and N. M. Plakida, Theor. Math. Phys. **152** (3), 1336 (2007).
6. N. Plakida, *High-Temperature Cuprate Superconductors: Experiment, Theory, and Applications* (Springer-Verlag, Berlin, 2010).
7. M. V. Sadovskii, Phys.—Usp. **44** (5), 515 (2001).
8. V. V. Val'kov and D. M. Dzebisashvili, J. Exp. Theor. Phys. **100** (3), 608 (2005).
9. V. V. Val'kov and A. A. Golovnya, J. Exp. Theor. Phys. **107** (6), 996 (2008).
10. V. J. Emery, Phys. Rev. Lett. **58**, 2794 (1987).
11. C. M. Varma, S. Schmitt-Rink, and E. Abrahams, Solid State Commun. **62**, 681 (1987).
12. J. E. Hirsch, Phys. Rev. Lett. **59**, 228 (1987).
13. J. Zaanen and A. M. Oles, Phys. Rev. B: Condens. Matter **37**, 9423 (1988).
14. B. Lau, M. Berciu, and G. A. Sawatzky, Phys. Rev. Lett. **106**, 036401 (2011).
15. R. Zwanzig, Phys. Rev. **124**, 983 (1961).
16. H. Mori, Prog. Theor. Phys. **33**, 423 (1965).
17. A. Damascelli, Z. Hussain, and Z.-X. Shen, Rev. Mod. Phys. **75**, 473 (2003).
18. V. Borisenko, M. S. Golden, S. Legner, T. Pichler, C. Dürr, M. Knupfer, J. Fink, G. Yang, S. Abell, and H. Berger, Phys. Rev. Lett. **84**, 4453 (2000).
19. T. Yoshida, X. J. Zhou, T. Sasagawa, W. L. Yang, P. V. Bogdanov, A. Lanzara, Z. Hussain, T. Mizokawa, A. Fujimori, H. Eisaki, Z.-X. Shen, T. Kakeshita, and S. Uchida, Phys. Rev. Lett. **91**, 027001 (2003).
20. X. J. Zhou, T. Yoshida, D.-H. Lee, W. L. Yang, V. Brouet, F. Zhou, W. X. Ti, J. W. Xiong, Z. X. Zhao, T. Sasagawa, T. Kakeshita, H. Eisaki, S. Uchida, A. Fujimori, Z. Hussain, and Z.-X. Shen, Phys. Rev. Lett. **92**, 187001 (2004).
21. T. Yoshida, X. J. Zhou, D. H. Lu, Y. Ando, H. Eisaki, T. Kakeshita, S. Uchida, Z. Hussain, Z. X. Shen, and A. Fujimori, J. Phys.: Condens. Matter **19**, 125209 (2007).
22. B. O. Wells, Z. X. Shen, A. Matsuura, D. M. King, M. A. Kastner, M. Greven, and R. J. Birgeneau, Phys. Rev. Lett. **74**, 964 (1995).
23. D. S. Marshall, D. S. Dessau, A. G. Loeser, C.-H. Park, A. Y. Matsuura, J. N. Eckstein, I. Bozovic, P. Fournier, A. Kapitulnik, W. E. Spicer, and Z.-X. Shen, Phys. Rev. Lett. **76**, 4841 (1996).

24. K. M. Shen, F. Ronning, D. H. Lu, W. S. Lee, N. J. C. Ingle, W. Meevasana, F. Baumberger, A. Damascelli, N. P. Armitage, L. L. Miller, Y. Kohsaka, M. Azuma, M. Takano, H. Takagi, and Z.-X. Shen, Phys. Rev. Lett. **93**, 267002 (2004); K. M. Shen, F. Ronning, W. Meevasana, D. H. Lu, N. J. C. Ingle, F. Baumberger, W. S. Lee, L. L. Miller, Y. Kohsaka, M. Azuma, M. Takano, H. Takagi, and Z.-X. Shen, Phys. Rev. B: Condens. Matter **75**, 075115 (2007).
25. F. Ronning, C. Kim, K. M. Shen, N. P. Armitage, A. Damascelli, D. H. Lu, D. L. Feng, Z.-X. Shen, L. L. Miller, Y.-J. Kim, F. Chou, and I. Terasaki, Phys. Rev. B: Condens. Matter **67**, 035113 (2003).
26. J. G. Tobin, C. G. Olson, C. Gu, J. Z. Liu, F. R. Sohal, M. J. Fluss, R. H. Howell, J. C. O'Brien, H. B. Radousky, and P. A. Sterne, Phys. Rev. B: Condens. Matter **45**, 5563 (1992).
27. K. Gofron, J. C. Campuzano, H. Ding, C. Gu, R. Liu, B. Dabrowski, B. W. Veal, W. Cramer, and G. Jennings, J. Phys. Chem. Solids **54**, 1193 (1993).
28. A. A. Abrikosov, J. C. Campuzano, and J. C. Gofron, Physica C (Amsterdam) **214**, 73 (1993).
29. D. S. Dessau, Z. X. Shen, D. M. King, D. S. Marshall, L. W. Lombardo, P. H. Dickinson, A. G. Loeser, J. DiCarlo, C.-H. Park, A. Kapitulnik, and W. E. Spicer, Phys. Rev. Lett. **71**, 278 (1993).
30. D. M. King, Z. H. Shen, D. S. Dessau, D. S. Marshall, C. H. Park, W. E. Spicer, J. L. Peng, Z. Y. Li, and R. L. Greene, Phys. Rev. Lett. **73**, 3298 (1994).
31. P. Aebi, J. Osterwalder, P. Schwaller, L. Schlapbach, M. Shimoda, T. Mochiku, and K. Kadowaki, Phys. Rev. Lett. **72**, 2757 (1994).
32. A. G. Loeser, Z. X. Shen, D. S. Dessau, D. S. Marshall, C. H. Park, P. Fournier, and A. Kapitulnik, Science (Washington) **273**, 325 (1996).
33. H. Ding, T. Yokoya, J. C. Campuzano, T. Takahashi, M. Randeria, M. R. Norman, T. Mochiku, K. Kadowaki, and J. Giapintzakis, Nature (London) **382**, 51 (1996).
34. H. Ding, M. R. Norman, T. Yokoya, T. Takeuchi, M. Randeria, J. C. Campuzano, T. Takahashi, T. Mochiku, and K. Kadowaki, Phys. Rev. Lett. **78**, 2628 (1997).
35. G. Shirane, Y. Endoh, R. J. Birgeneau, M. A. Kastner, Y. Hidaka, M. Oda, M. Suzuki, and T. Murakami, Phys. Rev. Lett. **59**, 1613 (1987).
36. M. Inui, S. Doniach, and M. Gabay, Phys. Rev. B: Condens. Matter **38**, 6631 (1988).
37. J. F. Annet, R. M. Martin, A. K. McMahan, and S. Satpathy, Phys. Rev. B: Condens. Matter **40**, 2620 (1989).
38. J. Kondo and K. Yamaji, Prog. Theor. Phys. **47**, 807 (1972).
39. H. Shimahara and S. Takada, J. Phys. Soc. Jpn. **60**, 2394 (1991).
40. A. F. Barabanov and V. M. Berezovskii, J. Exp. Theor. Phys. **79** (2), 344 (1994).
41. A. F. Barabanov, A. A. Kovalev, O. V. Urazaev, A. M. Belemuk, and R. Hayn, J. Exp. Theor. Phys. **92** (4), 677 (2001).
42. M. Ogata and H. Fukuyama, Rep. Prog. Phys. **71**, 036501 (2008).
43. O. A. Starykh, O. F. A. Bonfim, and G. F. Reiter, Phys. Rev. B: Condens. Matter **52**, 12534 (1995).
44. A. F. Barabanov, A. V. Mikheenkov, and A. V. Shvartsberg, Theor. Math. Phys. **168** (3), 1192 (2011).
45. B. Keimer, N. Belk, R. J. Birgeneau, A. Cassanho, C. Y. Chen, M. Greven, M. A. Kastner, A. Aharony, Y. Endoh, R. W. Erwin, and G. Shirane, Phys. Rev. B: Condens. Matter **46**, 14034 (1992).
46. V. Barzykin and D. Pines, Phys. Rev. B: Condens. Matter, **52**, 13585 (1995).
47. M. M. Korshunov and S. G. Ovchinnikov, Eur. Phys. J. B **57**, 271 (2007).
48. R. O. Kuzian, R. Hayn, A. F. Barabanov, and L. A. Maksimov, Phys. Rev. B: Condens. Matter **58**, 6194 (1998).

Translated by N. Wadhwa